Title

The Effect of Contact Area on the Permeability of Fractures

Authors

Chen, D W
Zimmerman, R W
Cook, N G W

Publication Date

1989-06-01

Lawrence Berkeley Laboratory
UNIVERSITY OF CALIFORNIA

EARTH SCIENCES DIVISION

Presented at the 30th U.S. Symposium on Rock Mechanics, Morgantown, WV, June 19–21, 1989, and to be published in the Proceedings

The Effect of Contact Area on the Permeability of Fractures

D.W. Chen, R.W. Zimmerman, and N.G.W. Cook

June 1989

Prepared for the U.S. Department of Energy under Contract Number DE-AC03-76SF00098.

LBL-27357

The Effect of Contact Area on the Permeability of Fractures

D. W. Chen, R. W. Zimmerman, and N. G. W. Cook

Earth Sciences Division
Lawrence Berkeley Laboratory
1 Cyclotron Road
Berkeley, California 94720

June 1989

This work was supported by the Manager, Chicago Operations, Repository Technology and Transportation Program, of the U.S. Department of Energy under Contract No. DE-AC03-76SF00098.

The Effect of Contact Area on the Permeability of Fractures

D. W. Chen, R. W. Zimmerman, and N. G. W. Cook

Earth Sciences Division
Lawrence Berkeley Laboratory
1 Cyclotron Road
Berkeley, California 94720

ABSTRACT

The permeability of a rock fracture is controlled primarily by the geometry of its void space. In order to focus on the tortuosity induced by the contact area, we consider an idealized fracture consisting of two parallel plates propped open by isolated asperities. Boundary-element calculations, analogue electrical conductivity measurements, and an effective medium approximation are used to study the permeability of fractures with circular, elliptical, and irregular asperity shapes.

1 INTRODUCTION

In many geological formations with low matrix permeability, fluid flow takes place predominantly through fractures. Fracture-dominated flow has become increasingly important in various problems of geotechnical interest, particularly those involving underground waste isolation. In some cases flow takes place through a particular fracture or fault, while in other cases the flow is through a network of fractures. In either case, an understanding of the permeability of single fractures is required.

The permeability of a naturally occurring rock fracture depends principally on the geometry of the void space. The geometry of a typical fracture consists of regions where the two rock surfaces are in contact (asperities), surrounded by regions where the two surfaces are separated by a distance (known as the aperture, h) that may vary from point to point. When fluid flows through such a fracture, it not only must flow around the contact areas, but also has a tendency to preferentially flow through the channels with the largest apertures (Brown 1987), since hydraulic conductance is proportional to h^3. In order to successfully model this process, both effects must be taken into account. In this paper, however, attention will be focused on the tortuosity induced by the contact regions. We therefore consider idealized fractures consisting of two parallel surfaces, with isolated regions of contact. Numerical and analytical methods will be used to relate the decrease in permeability (relative to that of unobstructed flow between parallel plates) to the amount of contact area, and the geometrical structure of the contact areas.

2 FORMULATION OF PROBLEM

The flow of a Newtonian fluid (such as water) through a fracture is governed by the Navier-Stokes equations. Exact solutions for specific geometries are extremely difficult to obtain; the exact solution for flow between two parallel plates under a uniform pressure gradient, however, is known (Schlichting 1968). The velocity profile for this flow is parabolic, with zero velocity at the upper and lower surfaces to satisfy the no-slip boundary condition. The total fluid flux Q (per unit depth of fracture into page on Figure 1) is found by integrating the velocity across the thickness of the channel. This leads to the familiar cubic law $Q = h^3 G/12\mu$, where $G = |\nabla P|$ is the magnitude of the pressure gradient, and μ is the viscosity of the fluid.

For a fracture that is modeled as two parallel plates propped open by discrete areas of contact (Figure 1), the flow cannot be everywhere parallel to the overall pressure gradient, since the fluid must follow a tortuous path as it circumvents the obstacles. If the flow rates are suitably low, and if the aperture h is small relative to the characteristic distance L between the contact areas (Figure 1), the flow can be well approximated by "Hele-Shaw" flow (Schlichting 1968, p. 114). The precise constraint on the velocity is that $Re^* = \rho U h^2/\mu L << 1$, where Re^* is the reduced Reynolds' number, and U is the mean velocity magnitude. In Hele-Shaw flow, the fluid still has a parabolic velocity profile, and the velocity vector $\vec{u}$ at each point is still in the direction of decreasing pressure, but the local pressure gradient is not necessarily the same as the overall macroscopic pressure gradient. The velocity profile for this type of flow is given by

$$\vec{u} = \frac{-\nabla P}{2\mu} z\,(z-h)\,, \tag{1}$$

where z is the transverse coordinate measured from the bottom wall. The pressure is found by solving the two-dimensional Laplace equation in the region of the $x-y$ plane exterior to the obstacles, i.e.

$$\nabla^2 P(x,y) = 0. \tag{2}$$

Since there can be no flow into or out of the obstacles, the pressure field must satisfy $\partial P/\partial n = 0$ along the obstacle boundaries, where n is the outward unit normal vector. The external boundaries are typically either no-flow or constant-pressure boundaries (Figure 2). Note that while the obstacles are correctly treated as being impermeable, it is not possible to impose the no-slip boundary condition along these surfaces, since the Laplace equation is of lower order than the Navier-Stokes equations. This incorrect boundary condition introduces an error which is on the order of (h/L), and which therefore should be negligible for many applications. For example, typical values of h for fractures in crystalline rock are on the order of $10-100$ μm, while asperity separations L are usually on the order of millimeters (Pyrak-Nolte et al. 1987).

3 METHODS OF ANALYSIS

3.1 Boundary-element analysis

The boundary-value problem described above can be solved for general obstacle shapes using any of the numerical schemes that have been constructed to treat Laplace's equation. We use a boundary-element method to solve the Laplace equation in square regions containing contact areas of various shapes (Figure 2). Fixed pressures are maintained on two opposing edges of the region, while the other two sides

are taken to be no-flow boundaries. The boundary-element method has certain advantages over finite-differences or finite-elements for this type of problem, since it requires discretization only of the boundaries of the problem, instead of the entire flow region. Briefly described, the boundary-element method utilizes "point-source" type solutions to the partial differential equation, and superimposes them to satisfy the boundary conditions in some average or approximate sense. Details of the method, and some computer programs, can be found in Brebbia (1978). The boundary-element calculations yield the pressure distribution throughout the flow region. The velocity vector can be found from equation (1), after which the total flux through the region is found by integrating the normal component of the velocity vector across one of the constant-pressure boundaries.

3.2 Analogue measurements

Since the fluid flow is described by Laplace's equation, with the contact areas serving as impermeable boundaries, this problem is analogous to the flow of electrical current in a thin sheet with holes punched in it. Since the holes obstruct the flow of electrical current, they play the role of the asperity obstacles. Experiments were therefore carried out on such sheets to measure the overall electrical conductivity (which is the analogue of the fracture permeability), in order to validate the numerical code. For these experiments, a thin sheet of conductive paper is cut into a square, and a strip of metallic paint is applied to two opposing edges. Since the conductivity of the paint is much higher than that of the paper, these edges will therefore be lines of constant potential. Holes which have the desired shapes, sizes and locations are cut out of the sheet, and the overall conductance is measured with an ohm-meter. Since resistance measurements can be made very accurately, this method is limited only by the precision with which the holes can be cut.

3.3 Effective-medium theory

The problem outlined above is a typical one in the area of effective properties of heterogeneous media. The unobstructed areas between the obstacles are regions of permeability K_o (say), while the obstacles are regions of zero permeability, and it is desired to determine the effective macroscopic permeability K^* that can represent flow through the fracture on a length scale large enough to cover many asperities. Since this problem is governed by Laplace's equation, the method introduced by Maxwell (see Carslaw & Jaeger 1959, p. 425) to predict the overall electrical conductivity of composite media can be applied. In the terminology of the present problem, this method considers the decrease in flow due to a single obstacle of known size and shape, averages this effect over all shapes and orientations of the obstacles, and then equates the resulting decrease in flux to that which would be caused by a single circular "obstruction" which has some effective permeability K^*. Walsh (1981) applied this method to a fracture with "randomly" located circular obstructions; we extend this method to cases where the obstacles are elliptical in shape, with random orientations.

4 RESULTS

4.1 Circular obstructions

In general, the effective fracture permeability will depend on both the shape of the obstructions, and their location and orientation. The simplest case to consider is that of circular obstructions, for which the issue of orientation is not relevant; this is also the only case for which analytical estimates of the permeability have been derived (Walsh 1981). Walsh used Maxwell's effective medium approach, along with the solutions for the potential fields surrounding circular inclusions (Carslaw & Jaeger

1959, p. 426), to derive the following expression for the effective permeability:

$$\frac{K^*}{K_o} = \frac{1-c}{1+c}, \tag{3}$$

where c is the fractional contact area of the fracture. Walsh interpreted this result as applying to "randomly located" obstructions. However, the Maxwell formalism cannot account for correlations in the locations of the asperities. Furthermore, any deviation from randomness would introduce a second-order effect that is probably not felt at the low values of c found in naturally occurring fractures, which are usually less than 25% (Tsang & Witherspoon 1981).

Boundary-element calculations were carried out for fractures with circular obstructions arranged in both hexagonal (Figure 3) and square arrays, for values of c ranging from 0 to 0.25. When the obstructions have the sort of symmetry exhibited by these arrangements, it suffices to perform the calculations in a "unit cell" formed by the imaginary grid of intersecting no-flow and constant pressure lines. Perhaps surprisingly, in light of its approximate nature, Walsh's expression was found to be extremely accurate. Note that the hexagonal array should lead to isotropic permeability variations, while the square array should not. However, the effect of asperity location was less than 1% at these values of c, and so it seems that the assumption of randomness can be relaxed when applying Walsh's expression. As an additional check on the accuracy of the boundary-element calculations, analogue measurements were also carried out. The measured electrical conductivities (see Figure 3) also agreed very closely with equation (3).

4.2 Elliptical obstructions

Since the Walsh-Maxwell effective medium approach works very well for circular obstructions, it is worthwhile to extend it to more general shapes. One general shape that is often used in modeling various physical properties of rocks is the ellipse (Zimmerman 1984). Although it could be said that the ellipse, as well as the circle, are both too idealized to represent real asperities, the ellipse has the advantage that by varying the aspect ratio, one can achieve different values of the perimeter-to-area ratio.

The basic problem that must be solved in order to apply this approach to elliptical obstructions is Laplace's equation in the region exterior to an ellipse, with a uniform potential gradient at infinity, and no flow across the boundary of the ellipse. The ellipse has an arbitrary angular orientation with respect to the imposed potential; the effect on the flow is then averaged over all (equally likely) orientations. The solution to this problem can be found in Batchelor (1967), where it was derived in the context of inviscid flow across an ellipse. Note that this is mathematically equivalent to the our problem, although the physical analogy is not so direct, since in the inviscid problem the velocity potential which satisfies equation (2) is not equal to the pressure. While the intermediate algebraic steps are somewhat complicated, the final expression for the effective permeability is only slightly different in form from equation (3) for circular obstructions:

$$\frac{K^*}{K_o} = \frac{1-\beta c}{1+\beta c}, \qquad \text{where} \quad \beta = \frac{(1+\alpha)^2}{4\alpha}, \tag{4}$$

and the aspect ratio α (≤ 1) is defined as the ratio of the minor to major axis. Note that for circular obstructions, $\alpha = 1$, and $\beta = 1$, so that expression (4) for elliptical obstructions reduces to Walsh's expression for circular obstructions.

The beta factor defined in equation (4) is always greater than unity, and monotonically increases as the ellipse becomes more elongated. Hence the $K^*(c)/K_o$ curves for elliptical obstructions will always lie below Walsh's curve. (In fact, since circular "inclusions" usually lead to upper or lower bounds in effective medium problems, it is reasonable to expect that Walsh's result is an upper bound with respect to all possible geometries). The predictions of the effective medium theory for $\alpha=0.2$ are shown in Figure 4, where they are compared to boundary-element calculations. The elliptical obstacles were generated by placing them on an hexagonal array (as in Figure 3), and then assigning to each ellipse a randomly chosen angular orientation. Over the range of contact areas shown in the figure, the effective medium estimates are very accurate. (Note that a contact area of 4% consisting of ellipses with $\alpha=0.2$ corresponds to the same number of obstacles per unit area as a 20% concentration of circular obstacles). Due to the extremely laborious and painstaking procedure required to cut out the holes in conductive sheet, only one analogue measurement was made; this value (Figure 4) was also in relatively close agreement with the predictions of equation (4).

4.3 Irregular obstructions

The shapes of asperity obstructions found in real rock fractures are of course more irregular than circles or ellipses. We have therefore used our boundary-element code to study flow around irregularly shaped obstacles such as that shown in Figure 5. These patterns are generated by breaking up the square into a 64×64 rectangular grid, and assigning each grid block to be either an obstruction zone or a flow zone. The parameter that can be altered when generating these patterns is the correlation-length parameter (see Coakley 1989). As expected, the calculated permeabilities lie below equation (3). These permeabilities can be fit fairly well by using the elliptical obstruction model (equation (4)) along with a value of $\alpha=0.25$. It can be conjectured that

this value of α is somehow related to the perimeter-to-area ratio of the irregular obstruction pattern; this possibility is currently being investigated.

5 CONCLUSIONS

Numerical, analogue and analytical methods have been used to investigate the effect of contact area geometry on the permeability of a fracture. To isolate the effect of contact area, the fracture aperture has been assumed constant in the regions between the asperities. For obstacles that are circular in the plane of the fracture, the expression derived by Walsh (1981) using a Maxwell-type effective medium approximation (equation (3)) was found to be very accurate for contact areas up to at least 25%. The Walsh-Maxwell approach was extended to randomly oriented obstacles of elliptical shape (equation (4)), with the results verified numerically for certain values of the aspect ratio and percentage contact area. Fractures with more irregular contact area geometries were also studied using the boundary-element approach. Such fractures had permeabilities that were lower (by as much as 30%) than would be predicted by Walsh's expression, but which could be fit very well by the effective medium approximation if an equivalent aspect ratio is used.

ACKNOWLEDGEMENTS

This work was carried out under U.S. Department of Energy Contract DE-AC03-76SF00098. The authors thank Larry Myer and Peter Persoff of LBL for reviewing this paper.

REFERENCES

Batchelor, G.K. 1967. *Introduction to Fluid Dynamics,* Cambridge: Cambridge University Press.

Brebbia, C.A. 1978. *The Boundary Element Method for Engineers,* London: Pentech Press.

Brown, S.R. 1987. Fluid flow through rock joints: the effect of surface roughness. *J. Geophys. Res.* **92:** 1337-1347.

Carslaw, H.S. & J.C. Jaeger 1959. *Conduction of Heat in Solids.* Oxford: Oxford University Press.

Coakley, K. 1989. *Spatial Statistics for Predicting Flow through a Single Rock Fracture.* Ph.D. thesis, Stanford University.

Pyrak-Nolte, L.J., L.R. Myer, N.G.W. Cook & P.A. Witherspoon 1987. In G. Herget & S. Vongpaisal (eds.), *Proc. 6th Int. Cong. Rock Mech.,* pp. 225-231. Rotterdam: Balkema.

Schlichting, H. 1968. *Boundary-Layer Theory, 6th Ed.* New York: McGraw-Hill.

Tsang, Y.W. & P.A. Witherspoon 1981. Hydromechanical behavior of a deformable rock fracture subject to normal stress. *J. Geophys. Res.* **86:** 9287-9298.

Walsh, J.B. 1981. The effect of pore pressure and confining pressure on fracture permeability. *Int. J. Rock Mech. Min. Sci & Geomech. Abstr.* **18:** 429-435.

Zimmerman, R.W. 1984. *The Effect of Pore Structure on the Pore and Bulk Compressibilities of Consolidated Sandstones.* Ph.D. thesis, University of California at Berkeley.

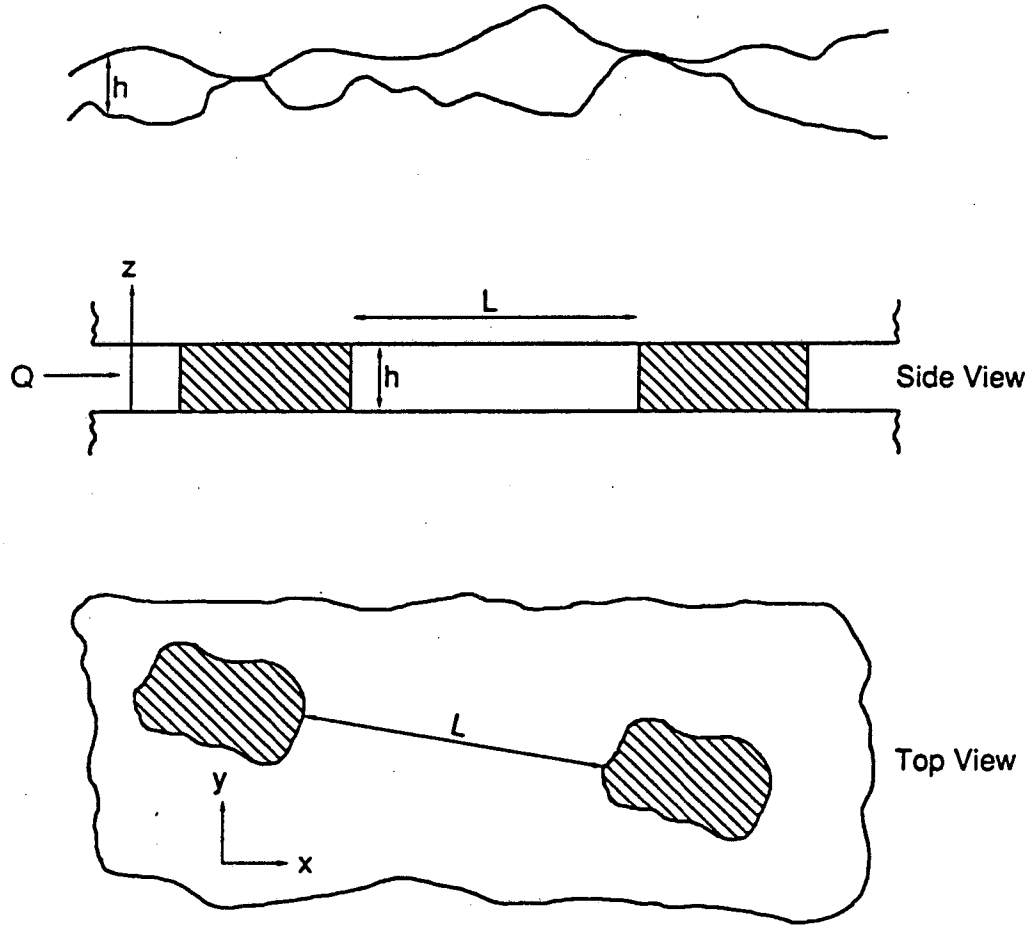

Figure 1. Top: Side view of a rock fracture. Middle and bottom: idealized fracture with parallel walls and isolated asperities.

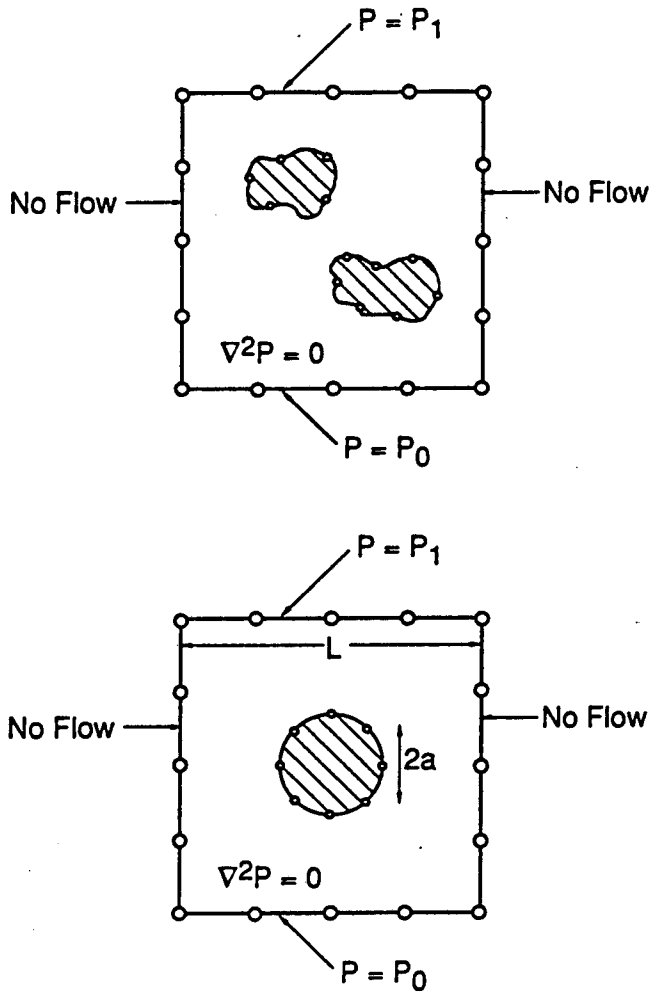

XBL 889-10455
T.I.D. Cricket Draw
9/29/88

Figure 2. Schematic diagram of the basic computational problem, showing two asperities, the no-flow and constant-pressure boundaries, and the discrete nodal points used in the boundary-element calculations.

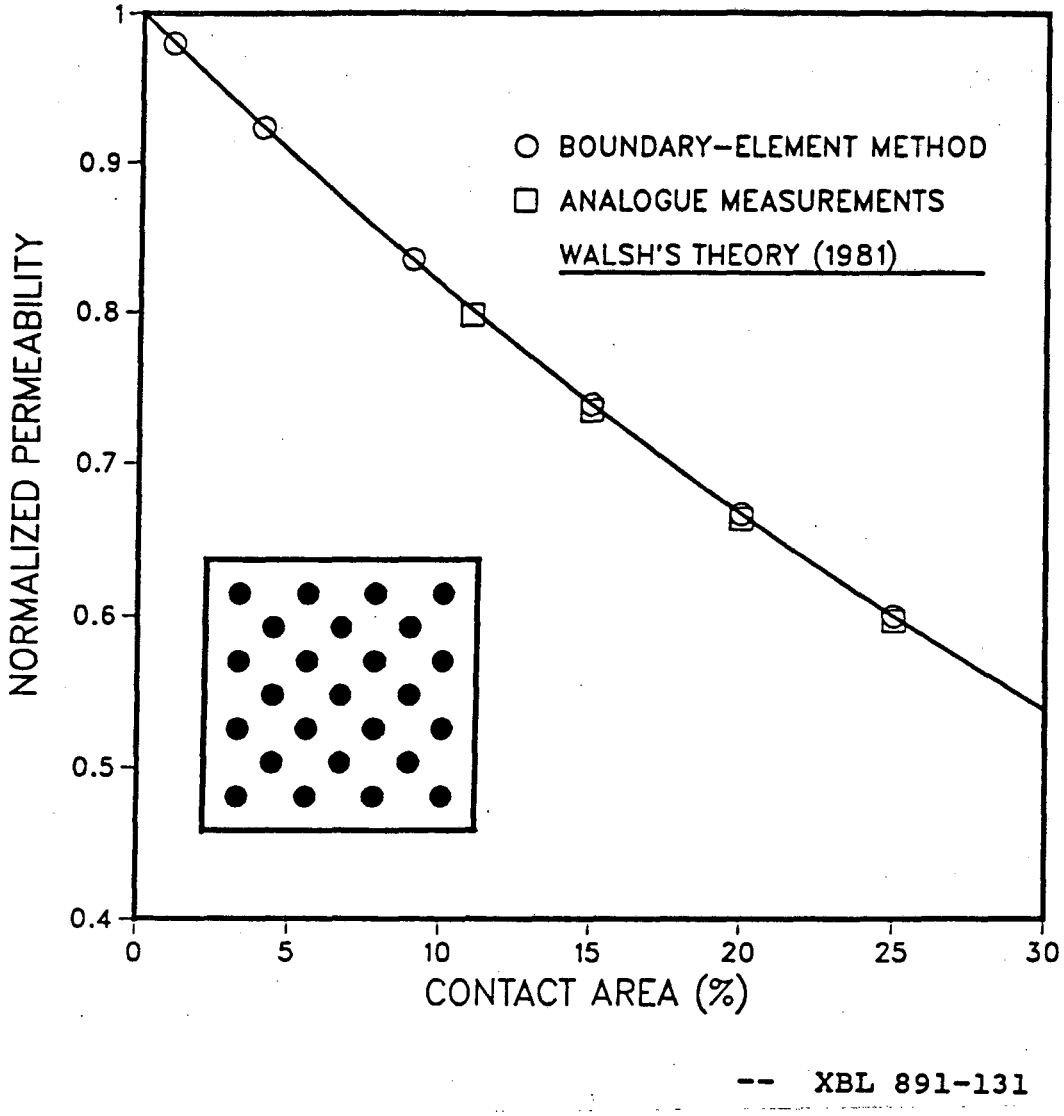

Figure 3. Normalized permeability of a fracture with circular asperities. Typical asperity geometry is shown in the inset.

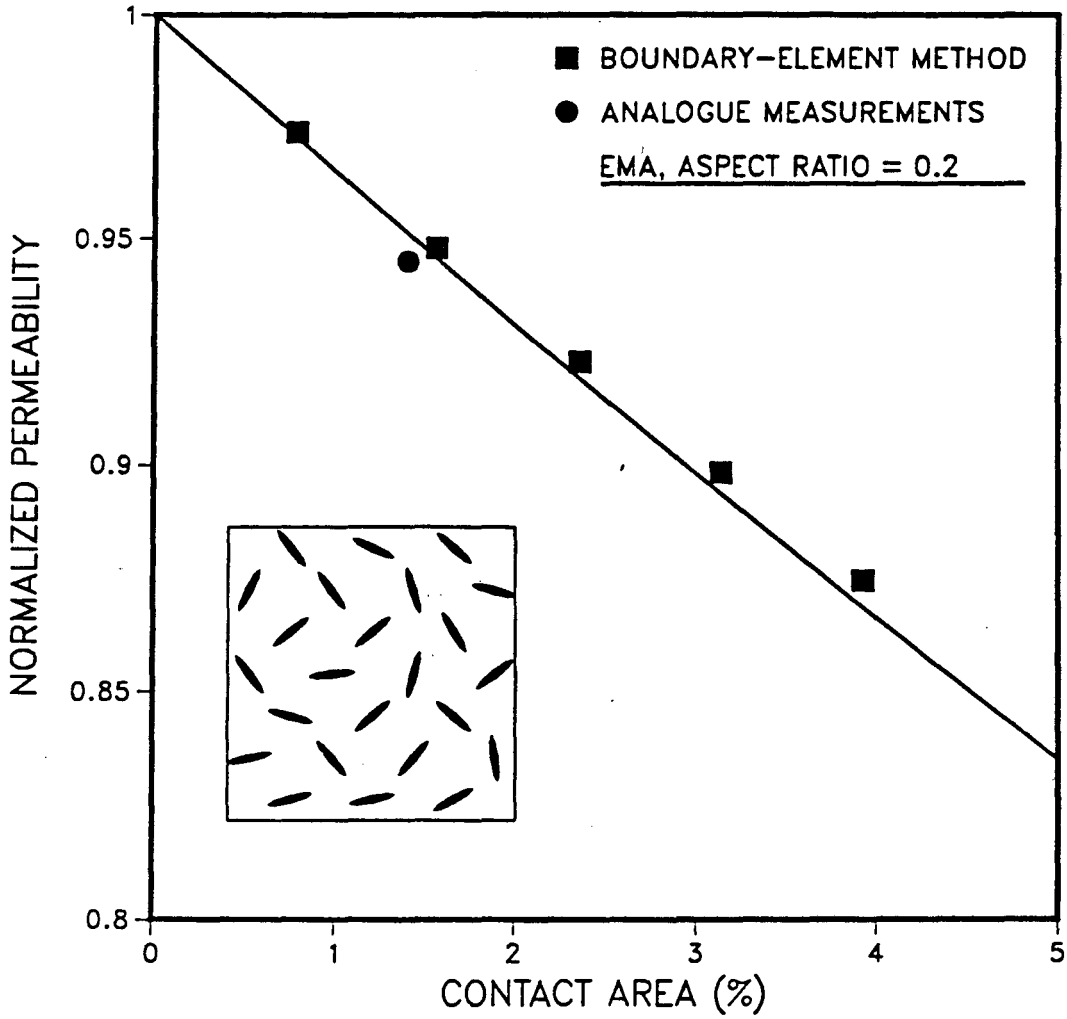

-- XBL 891-132 --

Figure 4. Normalized permeability of a fracture with elliptical asperities. Typical asperity geometry is shown in the inset.

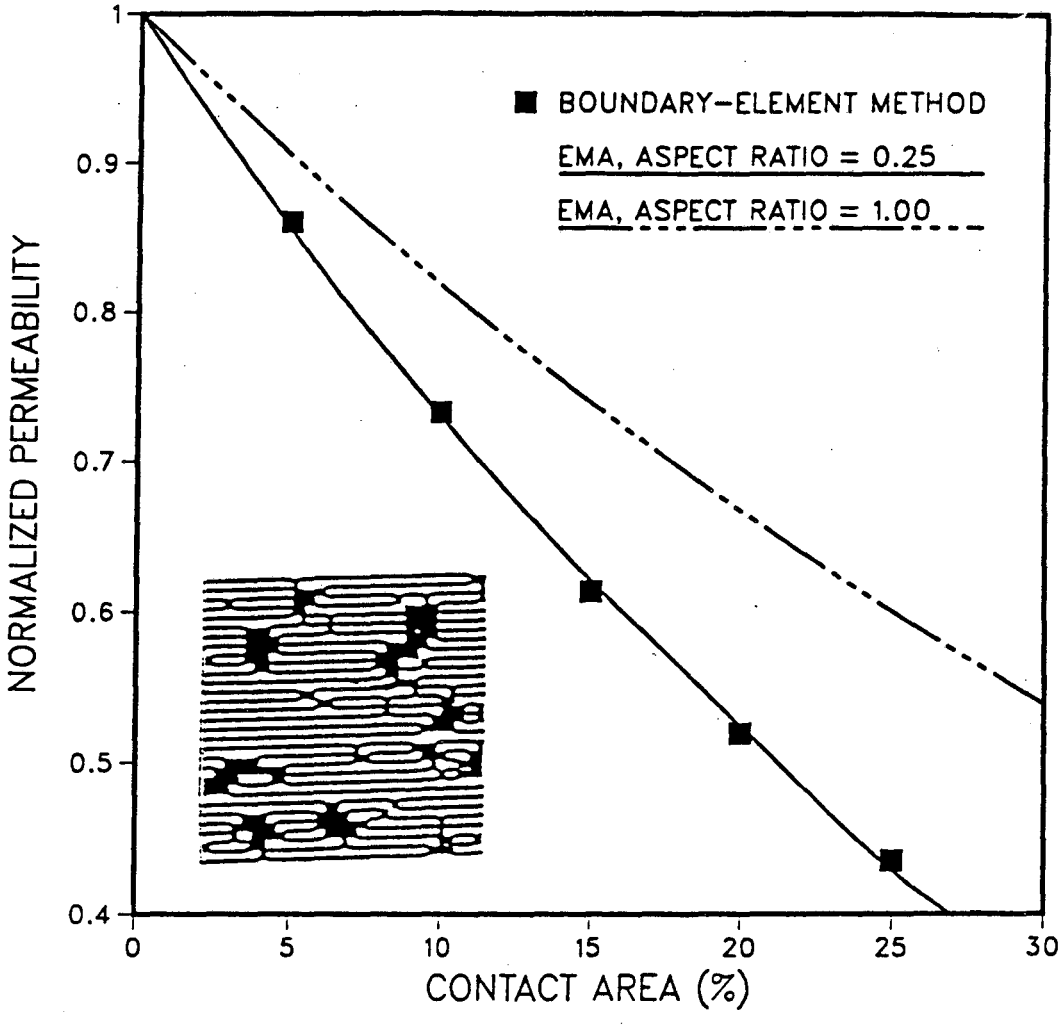

Figure 5. Normalized permeability of a fracture with irregular asperities. Example of asperity geometry is shown in the inset.

LAWRENCE BERKELEY LABORATORY
TECHNICAL INFORMATION DEPARTMENT
UNIVERSITY OF CALIFORNIA
BERKELEY, CALIFORNIA 94720